Deficiency of adipocyte fatty-acid-binding protein alleviates myocardial ischaemia/reperfusion injury and diabetes-induced cardiac dysfunction

Mi Zhou*, Yuqian Bao*, Haobo Li†, Yong Pan‡§, Lingling Shu‡§, Zhengyuan Xia†‡¶, Donghai Wu∥, Karen S.L. Lam‡§¶, Paul M. Vanhoutte‡¶**, Aimin Xu‡§¶**, Weiping Jia* and Ruby L.-C. Hoo‡§¶

*Department of Endocrinology and Metabolism, Shanghai Jiao Tong University Affiliated Sixth People's Hospital; Shanghai Diabetes Institute; Shanghai Key Laboratory of Diabetes Mellitus; Shanghai Clinical Center for Diabetes, Shanghai, China
†Department of Anesthesiology, LKS Faculty of Medicine, University of Hong Kong, Hong Kong
‡State Key Laboratory of Pharmaceutical Biotechnology, LKS Faculty of Medicine, University of Hong Kong, Hong Kong
§Department of Medicine, LKS Faculty of Medicine, University of Hong Kong, Hong Kong
¶Research Center of Heart, Brain, Hormone and Healthy Aging, LKS Faculty of Medicine, University of Hong Kong, Hong Kong
∥Key Laboratory of Regenerative Biology, Guangzhou Institute of Biomedicine and Health, Chinese Academy of Sciences, Guangzhou, China
**Department of Pharmacology and Pharmacy, LKS Faculty of Medicine, University of Hong Kong, Hong Kong

Abstract

Clinical evidence shows that circulating levels of adipocyte fatty-acid-binding protein (A-FABP) are elevated in patients with diabetes and closely associated with ischaemic heart disease. Patients with diabetes are more susceptible to myocardial ischaemia/reperfusion (MI/R) injury. The experiments in the present study investigated the role of A-FABP in MI/R injury with or without diabetes. Non-diabetic and diabetic (streptozotocin-induced) A-FABP knockout and wild-type mice were subjected to MI/R or sham intervention. After MI/R, A-FABP knockout mice exhibited reductions in myocardial infarct size, apoptotic index, oxidative and nitrative stress, and inflammation. These reductions were accompanied by an improved left ventricular function compared with the relative controls under non-diabetic or diabetic conditions. After diabetes induction, A-FABP knockout mice exhibited a preserved cardiac function compared with that in wild-type mice. Endothelial cells, but not cardiomyocytes, were identified as the most likely source of cardiac A-FABP. Cardiac and circulating A-FABP levels were significantly increased in mice with diabetes or MI/R. Diabetes-induced superoxide anion production was significantly elevated in wild-type mice, but diminished in A-FABP knockout mice, and this elevation contributed to the exaggeration of MI/R-induced cardiac injury. Phosphorylation of endothelial nitric oxide synthase (eNOS) and production of nitric oxide (NO) were enhanced in both diabetic and non-diabetic A-FABP knockout mice after MI/R injury, but diminished in wild-type mice. The beneficial effects of A-FABP deficiency on MI/R injury were abolished by the NOS inhibitor N^G-nitro-L-arginine methyl ester. Thus, A-FABP deficiency protects mice against MI/R-induced and/or diabetes-induced cardiac injury at least partially through activation of the eNOS/NO pathway and reduction in superoxide anion production.

Key words: adipocyte fatty-acid-binding protein, cardiac dysfunction, diabetes, endothelial nitric oxide synthase/nitric oxide (eNOS/NO) pathway, ischaemic heart disease, myocardial ischaemia/reperfusion

INTRODUCTION

Ischaemic heart disease is one of the leading causes of death worldwide [1]. The introduction of reperfusion therapy after acute ischaemia limits infarct size, but may paradoxically cause addi-tional cardiac damage and complications, known as myocardial ischaemia/reperfusion (MI/R) injury [2]. Diabetic patients are at high risk of ischaemic heart disease [3] and are more susceptible to MI/R injury, as evidenced by aggravated oxidative stress, cardiomyocyte apoptosis and myocardial dysfunction [4]. However,

the pathological link between diabetes and MI/R-induced cardiac injury is unclear.

Adipocyte fatty-acid-binding protein (A-FABP), an adipokine expressed in adipose tissues, activated macrophages as well as endothelial cells, is a key mediator of obesity-related metabolic deterioration and inflammation [5]. A-FABP can be released into the circulation [6] and its serum levels are elevated in obese patients with either Type 1 or Type 2 diabetes [7,8], and is positively associated with the key components of the metabolic syndrome, including hyperlipidaemia, hyperglycaemia, hypertension [6] and insulin resistance [7]. Both clinical and animal studies indicate that A-FABP is a key player in the pathogenesis of endothelial dysfunction and vascular diseases such as atherosclerosis [9]. Raised serum A-FABP levels are also closely associated with ischaemic heart disease [10,11].

Clinical findings suggest that A-FABP is implicated in cardiac dysfunction because raised serum A-FABP levels are associated with left ventricular diastolic dysfunction [12] and cardiac contractile dysfunction [13] in obese patients, or elevated left ventricular mass and reduced myocardial performance index in patients with obstructive sleep apnoea [14]. The circulating level of A-FABP independently correlates with the severity of heart failure in Chinese individuals [15] and is associated with increased risk of heart failure in older patients in the U.S.A. [16]. However, whether A-FABP is involved in the development of MI/R-induced cardiac dysfunction associated with diabetes remains elusive.

Endothelial cell–cardiomyocyte interactions play a critical role in the maintenance of cardiac function [17]. Endothelial cells express and release autocrine and paracrine factors such as nitric oxide (NO), endothelin-1, prostacyclin and angiotensin II, and provide a constant oxygen and nutrient supply for the cardiomyocytes [17]. Endothelial dysfunction in heart failure patients is associated with an elevated mortality [18]. *In vitro* studies suggest that A-FABP is implicated in endothelial dysfunction. Indeed, exogenous A-FABP suppresses endothelial nitric oxide synthase (eNOS) phosphorylation by inhibiting insulin-induced insulin receptor substrate 1 (IRS-1) and Akt activity, which in turn reduces NO production in endothelial cells [19,20]. By contrast, pharmacological inhibition of A-FABP confers protection against endothelial dysfunction in apolipoproteinE (ApoE) knockout (KO) mice [19] and in the pig [21].

The present study aimed to investigate whether A-FABP plays a pathophysiological role in MI/R-induced cardiac injury under both non-diabetic and diabetic conditions.

EXPERIMENTAL

Generation of A-FABP-deficient mice

The A-FABP KO targeting vector was constructed from genomic DNA fragments derived from a C57BL/6 genome, bacterial artificial chromosome clone. The targeting vector with a 3.5-kb 5′-upstream fragment from the ATG codon and a 5-kb 3′-downstream from the fourth exon of the *A-FABP* gene, encompassing luciferase and neomycin genes, was inserted into a pl253

vector. The linearized A-FABP KO targeting vector was electroporated into the embryonic stem cells of 129SV/J mice. The targeted clones were identified by PCR analysis and the A-FABP-targeted embryonic stem cells were microinjected into blastocysts and implanted into the uterus of C57BL/6N mice to generate chimaeras that were backcrossed with C57BL/6N mice to generate offspring. The genotypes of the pups were confirmed by PCR analysis using specific primers for wild-type (WT) A-FABP or A-FABP KO alleles (see Supplementary Table S1). A-FABP KO mice were crossed into a C57BL/6N background for at least six generations before the experiments. All mice were housed in a temperature-controlled facility (23 °C) with a 12-h light/12-h–dark cycle, and permitted free access to standard mouse chow (Purina) and water. All experimental protocols were approved by the Committee on the Use of Live Animals in Teaching and Research at the University of Hong Kong.

Diabetes induction

Mice 8 weeks old were injected intraperitoneally with a low dose (55 mg/kg) of streptozotocin (STZ, Alexa Biochemicals) dissolved in sterile 0.1 M citrate buffer for 5 consecutive days to induce diabetes. Control mice were injected with citrate buffer alone (pH 4.5). Mice with a blood glucose level higher than 300 mg/dl were considered to be diabetic. Blood glucose and body weight were monitored once weekly.

MI/R protocol

As previous studies demonstrated that there are gender differences in cardioprotection against global or myocardial ischaemia/reperfusion, and showed that female rats or mice are less susceptible than males to ischaemia/reperfusion injury [22], the MI/R experiments were performed using male mice. Both A-FABP KO mice and WT littermates were subjected to MI/R or sham intervention after 8 weeks of diabetes induction. MI/R was performed as described in [23]. In brief, age-matched WT and A-FABP KO mice with similar body weight and glucose levels were anaesthetized. Intratracheal intubation was performed to provide artificial ventilation by connecting the tubing to a TOPO Small Animal Ventilator (Kent Scientific) with a 0.3 ml tidal volume, 120 breaths/min and a 10–12 cm H_2O peak inspiratory pressure. A left thoracotomy was performed, and the left anterior descending artery (LAD) was ligated with an 8/0 silk suture. A 1-cm-long piece of polyethylene-10 tubing was placed on the heart between the LAD and the suture to facilitate reperfusion. The LAD was occluded completely for 30 min, and reperfused for 2 or 24 h (for cardiac function determination). Sham-operated control mice underwent the same surgical procedures, except that the suture placed under the left coronary artery was not tied. To study the effect of eNOS inhibition on MI/R- or diabetes-induced cardiac dysfunction, subgroups of WT and A-FABP KO mice were treated with the NOS inhibitor N^G-nitro-L-arginine methyl ester (L-NAME, Sigma–Aldrich) added to the drinking water at 1.5 mg/ml for 4 weeks.

Measurement of blood pressure

Systolic arterial blood pressure was determined non-invasively by the tail-cuff method using BP-2000 Blood Pressure Analysis

System (Visitech Systems) in conscious mice before they were subjected to MI/R or determination of cardiac function, after a training period of 5 days.

Determination of myocardial infarct size

At the end of reperfusion, the LAD was religated and 5% Evan's Blue Dye was injected directly into the left ventricle (LV) to delineate the ischaemic from the non-ischaemic area. The heart was then rapidly excised and cross-sectioned into 1-mm-thick sections, which were incubated with 1% 2,3,5-triphenyltetrazolium chloride (TTC, Sigma–Aldrich) in 0.2 mol/l phosphate solution for 20 min at 37°C to identify viable tissue. The infarcted area (unstained by TTC) and the area at risk (AAR, unstained by Evan's Blue Dye) were assessed using NIH Image J software. The infarct area was expressed as a percentage of the AAR.

Determination of cardiac function

Cardiac function was determined by invasive ventricular catheterization 24 h after reperfusion. A 1.4-Fr high-fidelity microtip catheter connected to a pressure transducer (Millar Instruments) was positioned into the LV through the right carotid artery to record left ventricular pressure changes. The left ventricular end-systolic pressure (LVESP), left ventricular end-diastolic pressure (LVEDP), maximal rate of pressure development (dP/dt_{max}) and maximal rate of decay of pressure ($-dP/dt_{min}$), representative of cardiac systolic and diastolic performance, were obtained using a PowerLab system (AD Instruments).

Determination of myocardial apoptosis

Myocardial apoptosis was detected by the terminal deoxynucleotidyl transferase-mediated dUTP nick-end labelling (TUNEL) assay using an *In Situ* Cell Death Detection Kit (Roche) according to the manufacturer's instructions. The cardiac sections including the entire MI/R areas were viewed at 488 nm excitation/512 nm emission. TUNEL-positive nuclei were counted in 20 random fields (×40) per animal and expressed as the percentage of total nuclei.

Measurement of superoxide anion production

In situ levels of myocardial superoxide anions were determined by dihydroethidium (DHE, Sigma–Aldrich) staining. DHE intercalates into DNA on oxidization by intracellular superoxide anions to produce fluorescent ethidium bromide. Frozen sections of left ventricular tissue were incubated with 7.5 μM DHE at 37°C for 30 min. Fluorescence images of ethidium bromide were obtained using a fluorescence microscope (BX41 System microscope; Olympus). The mean fluorescence intensities of DHE-labelled positive myocyte nuclei were quantified in each of five randomly selected fields and are shown as mean pixel intensity.

Determination of myocardial content of nitrotyrosine and NO products

The nitrotyrosine content, an index of peroxynitrite formation from $O_2{}^-$ and NO, was determined in MI/R tissue by chemiluminescent immunoassay using the competitive ELISA nitrotyrosine assay kit (Millipore). The total concentration of NO products was determined by quantification of two stable oxidized products of

NO, nitrites ($NO_2{}^-$) and nitrates ($NO_3{}^-$), using a nitrate/nitrite colorimetric assay kit (Cayman Chemical) according to the manufacturer's instructions.

Immunohistochemistry and immunofluorescence staining

Immunohistochemistry was performed on formalin-fixed paraffin-embedded (for A-FABP, troponin T and nitrotyrosine detection) or frozen (for CD31 detection) left ventricular tissue sections. After deparaffinization and rehydration, the sections were protected from endogenous peroxidases using 3% hydrogen peroxide for 30 min. Antigen retrieval was performed by incubating the slides in sodium citrate buffer, pH 6.0, at 95°C for 10 min. The slides were incubated with primary antibody overnight at 4°C in a humidity chamber, and the following primary antibodies were used: mouse anti-nitrotyrosine (Rockland), goat anti-A-FABP (R&D Systems) and mouse anti-troponin T (Thermo Scientific) at a dilution of 1:100. On the following day, the slides were incubated with anti-goat or anti-mouse horseradish peroxidase (HRP)-conjugated secondary antibodies (1:500 dilution, Sigma–Aldrich) at room temperature for 1 h, then developed with 3,3′-diaminobenzidine (DAB) solution (Sigma–Aldrich) and counterstained for nuclei with haematoxylin solution. For immunofluorescence staining, monoclonal rat anti-CD31 (BD Bioscience) at a dilution of 1:100 was also used (for frozen sections). Secondary antibodies were Alexa Fluor 594-conjugated chicken anti-goat IgG, Alexa Fluor 488-conjugated chicken anti-goat IgG, Alexa Fluor 594-conjugated rabbit anti-mouse IgG and Alexa Fluor 488-conjugated chicken anti-rat IgG (Molecular Probes). Primary antibody isotypes were used as negative controls. Nuclei were stained with 4′,6-diamidino-2-phenylindole (DAPI, Invitrogen). The mean fluorescence intensities of positively stained cells were quantified in each of five randomly selected fields.

Haematoxylin and eosin staining

Haematoxylin and eosin (H&E) staining was performed as described in [24]. Heart tissues were fixed overnight in buffered formaldehyde (10%) and embedded in paraffin. Sections that were 5-μm-thick were prepared. The air-dried sections were stained with H&E (Sigma–Aldrich) for histological analysis. The images were obtained at ×400 magnification using a microscope (BX41 System, Olympus) with a colour digital camera (Olympus Model DP72).

Western blotting

Protein samples from MI/R tissue homogenates were separated by SDS/PAGE, transferred onto PVDF membranes and probed with primary antibodies against A-FABP (R&D Systems), phospho-eNOS (Ser[1177], BD Biosciences), eNOS (BD Biosciences), inducible nitric oxide synthase (iNOS, Abcam) and β-actin (Cell Signaling Technology). The membranes were then incubated with HRP-conjugated secondary antibodies and developed with enhanced chemiluminescence reagents (GE Healthcare). The blot densities were quantified using NIH ImageJ software.

Quantitative real-time PCR

Total RNA was extracted from MI/R tissue using TRIzol reagent (Invitrogen). Total RNA (1 μg) was reverse-transcribed into cDNA using Improm-II reverse transcription kit (Promega). Quantitative real-time (qRT-PCR) was performed using SYBR Green Reagent (Qiagen) on an ABI Prism 7000 sequence detection system (Applied Biosystems). The primer sequences of inflammation-related genes used for reverse transcription–PCR, including tumour necrosis factor α (TNF-α), monocyte chemoattractant protein-1 (MCP-1), interleukin-6 (IL-6) and F4/80, are listed in Supplementary Table S2. The level of target gene expression was analysed using the $2^{(-\Delta\Delta C^T)}$ method and normalized against the glyceraldehyde-3-phosphate dehydrogenase (GAPDH) gene.

Biochemical analysis

Blood glucose was measured using an ACCU-Chek glucose meter (Roche). Serum A-FABP levels were measured using a mouse A-FABP ELISA kit (BioVendor Laboratory Medicine).

Statistical analysis

All data in the present study are expressed as means $\pm$ S.E.M. Data that were not normally distributed, as determined by the Kolmogorov–Smirnov test, were transformed logarithmically to produce normally distributed data before analysis. Statistically significant differences between groups were determined using one-way ANOVA analysis followed by Bonferroni's post-hoc test with SPSS version 16.0. Two-sided values of $P < 0.05$ were considered to indicate statistically significant differences.

RESULTS

Generation of systemic A-FABP KO mice

A-FABP KO mice were generated using a gene-targeting approach with a vector replacing exons 1–4 of the A-FABP gene with luciferase and neomycin genes (see Supplementary Figure S1a). Genotyping analysis using gene-specific primers was performed to identify the WT, A-FABP KO and heterozygous mice (see Supplementary Figure S1b). The absence of A-FABP protein expression in the heart of A-FABP KO mice was confirmed by immunoblotting and immunohistochemistry staining using goat anti A-FABP antibodies (see Supplementary Figures S1c and S1d).

A-FABP deficiency protects against MI/R-induced cardiac injury in both non-diabetic and diabetic mice

WT and A-FABP KO mice with STZ-induced diabetes developed rapid and persistent hyperglycaemia throughout the experimental period, which was accompanied by a markedly reduced body weight (see Supplementary Figure S2). No significant differences in body weight and blood glucose were found between WT and A-FABP KO mice in either the diabetic or the control groups.

MI/R resulted in significant myocardial infarction in both WT and A-FABP KO mice, which was exacerbated by diabetes. In both normal and diabetic mice, the percentage of the infarct area in the AAR was significantly reduced in A-FABP KO mice compared with their respective WT controls (non-diabetic WT: 47.64 $\pm$ 2.48 %; non-diabetic KO: 29.20 $\pm$ 1.86 %; diabetic WT: 56.67 $\pm$ 2.62 %; diabetic KO: 43.75 $\pm$ 2.15 %; $P < 0.01$) (Figure 1a). The extent of apoptosis in the AAR regions was determined by TUNEL staining. Consistent with the results of infarct size measurement, MI/R induced significant cardiac cell apoptosis, as indicated by the increased TUNEL positive-stained nuclei in WT and A-FABP KO mice compared with sham controls. MI/R-induced apoptosis was more severe in both types of mice under diabetic conditions (in WT mice: non-diabetic 54.4 % compared with diabetic 72.6 %, $P = 0.001$; in A-FABP KO mice: non-diabetic 35.1 % compared with diabetic 45.2 %, $P = 0.013$). A-FABP KO mice exhibited a significantly lower proportion of TUNEL-positive cells in their myocardium compared with their WT controls in both the non-diabetic and the diabetic groups (both $P < 0.01$) (Figure 1b), suggesting that A-FABP deficiency protects mice against MI/R-induced cardiac damage irrespective of the presence of diabetes.

A-FABP deficiency protects against diabetes- or MI/R-induced cardiac dysfunction

Severe hyperglycaemia was paralleled by impairment of both cardiac contractile and diastolic functions in WT mice, whereas diabetic A-FABP KO mice had a preserved cardiac function (Figures 2a–2d). MI/R induced significant cardiac systolic dysfunction as evidenced by reductions in LVESP (Figure 2a: in non-diabetic WT mice: sham 85.93 $\pm$ 2.06 mmHg compared with MI/R 55.18 $\pm$ 1.14 mmHg, $P < 0.001$; in non-diabetic KO mice: sham 84.51 $\pm$ 1.22 mmHg compared with MI/R 67.93 $\pm$ 2.41 mmHg, $P = 0.002$) and dP/dt_{max} (Figure 2c; in non-diabetic WT mice: sham 4561.60 $\pm$ 62.29 mmHg/s compared with MI/R 2877.65 $\pm$ 46.77 mmHg/s, $P < 0.001$; in non-diabetic KO mice: sham 4562.67 $\pm$ 195.81 mmHg/s compared with MI/R 3616.30 $\pm$ 87.88 mmHg/s, $P = 0.023$) in both WT and A-FABP KO mice, whereas the reductions were consistently less in A-FABP KO mice. Diabetes further exacerbated the MI/R-induced cardiac systolic dysfunction in both types of mice (in WT mice, LVESP reduced from 55.18 $\pm$ 1.14 to 42.09 $\pm$ 1.52 mmHg; in A-FABP KO mice, from 67.93 $\pm$ 2.41 to 54.67 $\pm$ 0.69 mmHg; dP/dt_{max} reduced from 2877.65 $\pm$ 46.77 to 1578.54 $\pm$ 88.33 mmHg/s in WT mice, and from 3616.30 $\pm$ 162.74 to 2945.27 $\pm$ 99.60 mmHg/s in A-FABP KO mice; all $P < 0.05$) (Figures 2a and 2c). MI/R induced a similar increment of LVEDP and reduction in $-$dP/dt_{min} in both WT and KO mice whereas diabetes further exaggerated the MI/R-induced impairment of cardiac diastolic function only in WT (all $P < 0.05$), but not in A-FABP KO mice (Figures 2b and 2d).

A-FABP deficiency attenuates MI/R- and diabetes-induced myocardial oxidative and nitrative stresses and inflammation

MI/R injury alone caused a severe disruption of the geometric alignment of cardiomyocytes in WT mice although the effect on A-FABP KO mice was mild. Diabetes alone also slightly altered the alignment of cardiomyocytes in WT mice but not in A-FABP KO mice. Under diabetic conditions, MI/R injury caused
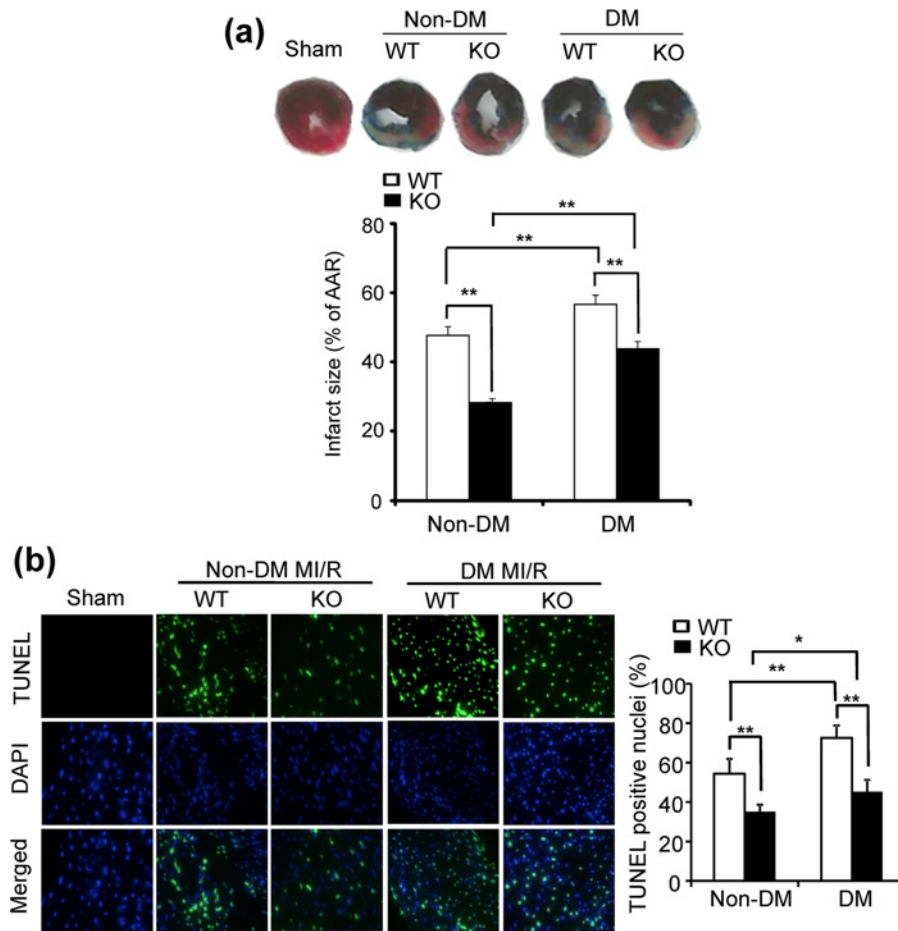
Figure 1   A-FABP deficiency attenuates myocardial infarction and apoptosis in MI/R-induced mice with (DM) or without (non-DM) diabetes

A-FABP-KO mice and their WT littermates were subjected to either vehicle (citrate buffer) or STZ injection to induce Type 1 diabetes followed by MI/R injury. (**a**) Myocardial infarct size was determined by Evan's Blue/TTC double staining. Upper panel: representative photomicrographs of heart sections obtained from MI/R-induced WT and A-FABP KO mice with or without DM. The blue-staining areas indicate normal myocardium, red-staining areas represent ischaemic but non-infarcted tissue, and unstained white areas indicate infarcted tissue. Lower panel: quantification of myocardial infarct size expressed as percentage of AAR, calculated as ischaemic area plus infarcted area divided by total area of the heart. (**b**) Diabetes- and MI/R-induced cardiac cell apoptosis was determined by TUNEL staining of the heart sections. TUNEL-stained apoptotic nuclei green and total nuclei were counterstained blue with DAPI. Magnification $\times 40$. Values are expressed as means $\pm$ S.E.M. $*P < 0.05$, $**P < 0.01$; $n = 5$–6.

a marked reduction in the number of cardiomyocytes in WT mice, as indicated by the reduced number of stained nuclei, whereas MI/R injury and diabetes induction had no synergistic effect on cardiac structural changes in A-FABP KO mice (Figure 3a).

The production of superoxide anion and formation of peroxynitrite were next accessed in cardiac tissue. DHE staining indicated that MI/R- or diabetes-induced superoxide anion production was significantly reduced in A-FABP KO mice compared with WT mice (Figure 3b). MI/R and diabetes synergistically increased superoxide anion production in both types of mice, but A-FABP KO mice consistently showed a significantly lower level when compared with WT mice (39–49% reduction in ethidium fluorescence intensity in KO mice compared with WT mice under MI/R, diabetes or diabetes+MI/R conditions). In addition, MI/R injury significantly increased nitrotyrosine formation in WT, but not in A-FABP KO, mice. Although diabetes alone did

not increase nitrotyrosine formation in both types of mice, diabetes significantly exaggerated MI/R-induced nitrotyrosine formation in WT mice, although that in A-FABP-deficient hearts was significantly attenuated as indicated by immunohistological staining (Figure 3c) and chemiluminescent protein quantification (Figure 3d).

Furthermore, MI/R induced a significant increase in cardiac expression of inflammatory cytokines, including TNF-α, MCP-1 and IL-6 in WT mice, whereas only the expression of MCP-1 was significantly enhanced in A-FABP KO mice, when compared with their respective sham control. Moreover, the MI/R-induced increase in inflammatory cytokines was significantly attenuated in the KO mice when compared with the respective WT mice (in WT mice, 3.37 ± 0.24-fold, 10.83 ± 1.30-fold and 8.17 ± 0.37-fold increased, respectively, compared with in A-FABP KO mice, 2.08 ± 0.12-fold, 4.99 ± 0.41-fold and 1.25 ± 0.13-fold
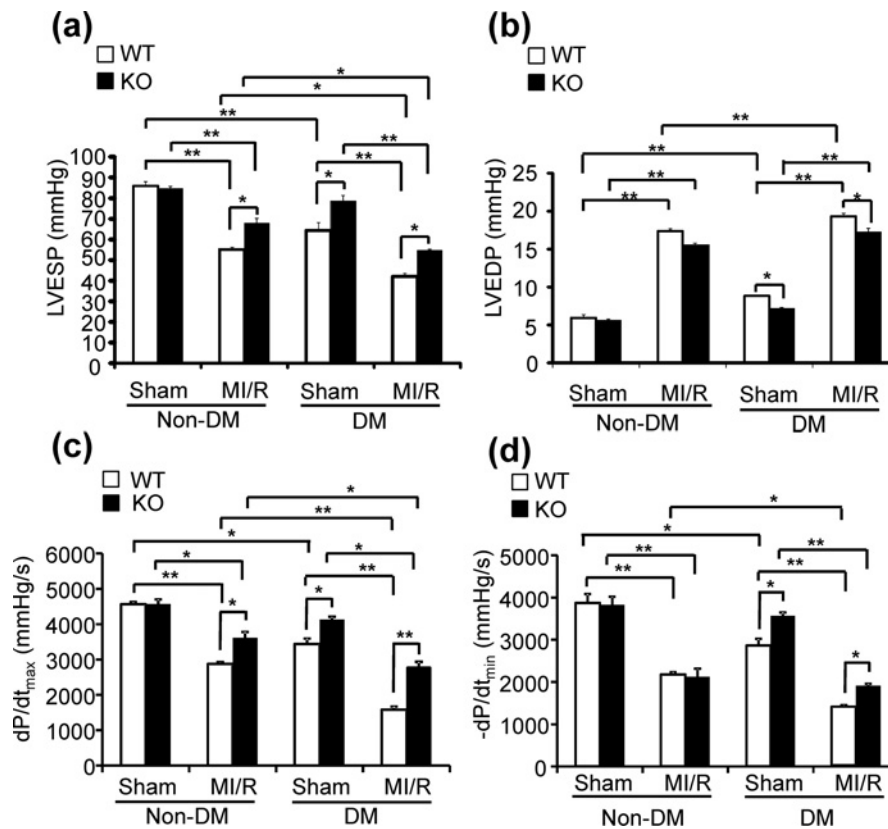
Figure 2 A-FABP deficiency attenuates cardiac dysfunction caused by diabetes induction or MI/R in mice with (DM) or without (non-DM) diabetes

Cardiac systolic and diastolic functions were determined by left ventricular catheterization as indicated by (**a**) LVESP, (**b**) LVEDP, (**c**) dP/dt_{max} and (**d**) −dP/dt_{min}. Values are expressed as means ± S.E.M. *$P < 0.05$, **$P < 0.01$; $n = 5$–6.

increased, respectively) (Figure 3e). Diabetes alone did not induce the cardiac expression of any inflammatory cytokine in both WT and A-FABP KO mice, but it significantly enhanced the MI/R-induced expression of TNF-α and IL-6 in WT mice, although the effect on that in A-FABP-KO mice was markedly diminished (Figure 3e). There was no significant increase in the cardiac mRNA expression level of F4/80 in the hearts of both WT and A-FABP KO mice after MI/R and/or diabetes induction, and the levels of F4/80 were similar between the two types of mice (see Supplementary Figure S3), suggesting that no significant macrophage infiltration had occurred. These data are consistent with previous findings that infiltration of macrophages starts at day 3 in the MI/R model [25]. Taken together, these results suggest that A-FABP deficiency attenuates MI/R-induced and/or diabetes-induced cardiac injury, at least partially, by reducing myocardial oxidative and nitrative stresses and inflammation.

The endothelium is the major cell source of cardiac A-FABP and its expression is induced further by MI/R and diabetes

Immunofluorescence staining demonstrated that A-FABP is expressed abundantly in the heart of WT mice (see Supplementary Figure S4a). Co-immunofluorescence staining showed that A-FABP co-localized only with the endothelial marker CD31, not with the cardiomyocyte marker troponin T (Figure 4a), suggesting that the major cell source of cardiac A-FABP is the endothelium. Western blot analysis also demonstrated that A-FABP was detected in adipose tissue (AT) and total heart lysate (THL) but not in primary cardiomyocytes (PCs) (Figure 4b). The mRNA expression of A-FABP in PCs was also undetectable by qRT-PCR (Figure 4c).

MI/R or diabetes caused a significant up-regulation of mRNA expression (Figure 4d) and protein presence (Figure 4e) of A-FABP in the heart tissue of WT mice. In addition, diabetes induced a higher expression of A-FABP than MI/R injury. Under diabetic conditions, MI/R further induced a mild but insignificant increase in mRNA and protein expression of cardiac A-FABP and its circulating level (see Supplementary Figure S4b). These data suggest that the elevated expression of A-FABP in diabetic mice subjected to MI/R is contributed to mainly by diabetes induction rather than MI/R injury. The cardiac expression of A-FABP was significantly higher in diabetic mice with MI/R compared with non-diabetic mice with MI/R (Figures 4d and 4e). A similar trend was observed for the serum A-FABP levels (see Supplementary Figure S4b), in line with previous clinical findings demonstrating raised circulating A-FABP levels in patients with diabetes [7,8] and/or ischaemic heart disease [10,11].
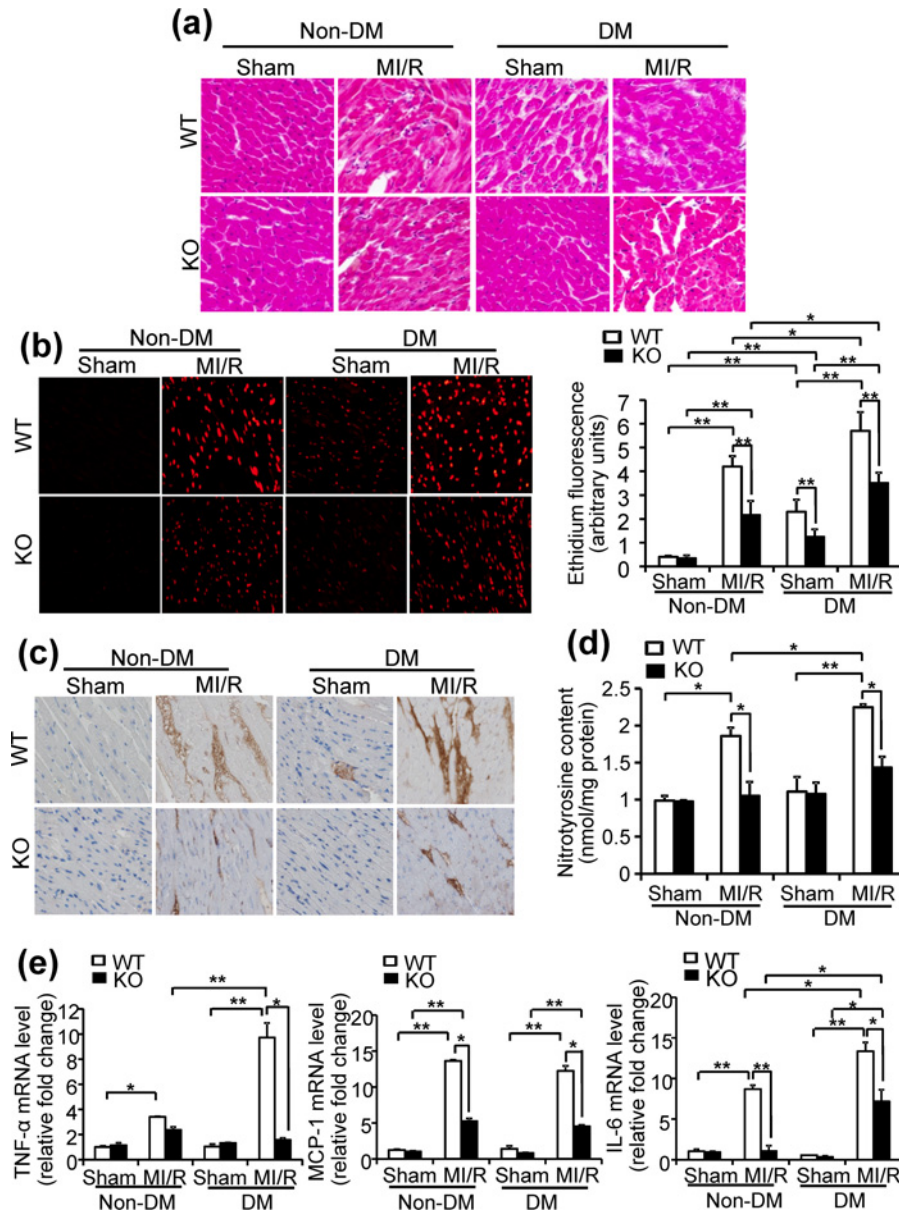
Figure 3   A-FABP deficiency alleviates MI/R- and diabetes-induced cardiac histological change, oxidative and nitrative stress, and inflammation

(**a**) Histological analysis of heart sections by H&E staining. (**b**) Cardiac superoxide anion production was determined by *in situ* DHE staining. The fluorescence of DHE-labelled positive nuclei (red) was calculated in each of five randomly selected fields and was expressed as mean pixel intensity. (**c**) Immunohistochemistry staining of cardiac nitrotyrosine in each of five randomly selected fields. Magnification $\times 40$. (**d**) Myocardial nitrotyrosine content was determined by chemiluminescence. (**e**) The mRNA abundance of pro-inflammatory cytokines TNF-α, MCP-1 and IL-6 in heart tissues was determined by qRT-PCR and normalized to the *GAPDH* gene. DM, diabetes mellitus. Values are expressed as means $\pm$ S.E.M. $*P < 0.05$, $**P < 0.01$; $n = 5$–6.

A-FABP deficiency enhances eNOS phosphorylation and NO production in the MI/R heart

The eNOS/NO pathway exerts cardioprotective effects against apoptosis and oxidative stress [26]. Exogenous A-FABP inhibits eNOS activation and NO production in cultured endothelial cells [20]. As A-FABP is expressed in cardiac endothelial cells and its expression is up-regulated by MI/R and diabetes, the next experiments examined whether A-FABP deficiency exerts

its cardioprotective effect by modulating the eNOS/NO pathway. In WT mice, MI/R caused a significant down-regulation of eNOS phosphorylation, and this detrimental effect was further exacerbated in diabetic mice, whereas diabetes alone did not alter eNOS phosphorylation (Figure 5a). By contrast, diabetes alone or MI/R injury induced a significant and similar increase in eNOS phosphorylation in A-FABP-deficient hearts, but MI/R injury did not further enhance eNOS phosphorylation in
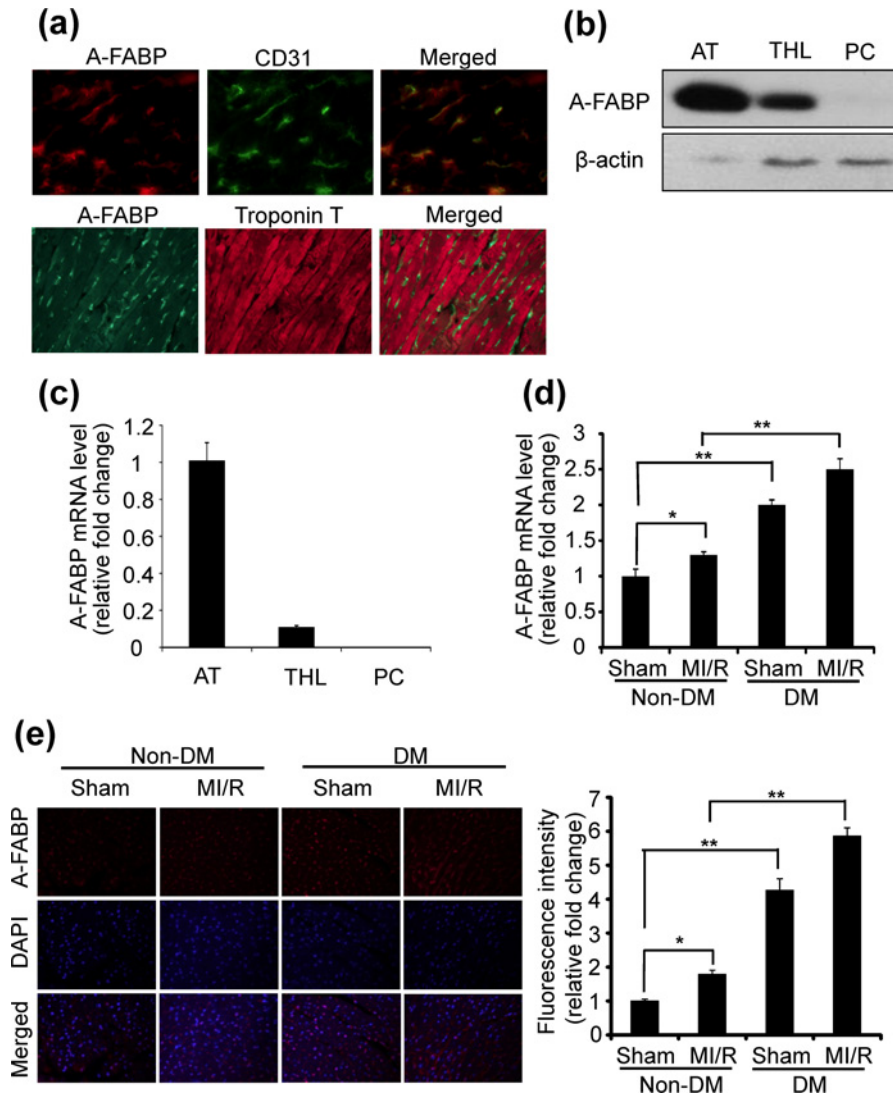
Figure 4   Endothelial cells are the major cell source of cardiac A-FABP, and its expression is further induced by MI/R and diabetes

(**a**) Co-immunofluorescence staining of cardiac A-FABP with the endothelial cell marker CD31 and the cardiomyocyte marker troponin T in the heart sections of WT mice. (**b**) Western blot analysis of A-FABP expression and (**c**) the mRNA abundance of A-FABP in AT, THL and PCs of WT mice. (**d**) The mRNA abundance of cardiac A-FABP in MI/R- and/or diabetes-induced WT mice was determined by qRT-PCR. (**e**) Immunofluorescence staining of cardiac A-FABP of MI/R- and/or diabetes-induced WT mice. Right panel: quantification of the fluorescence intensity. DM, diabetes mellitus. Values are expressed as means $\pm$ S.E.M. *$P < 0.05$, **$P < 0.01$; $n = 6$.

heart tissue of diabetic A-FABP KO mice (Figure 5b). Consistent with the increased eNOS phosphorylation, MI/R-subjected A-FABP-deficient hearts showed a significantly enhanced total NO production compared with those of WT controls under either control or diabetic conditions (Figure 5c, 1.60 ± 0.14 compared with 0.92 ± 0.16 nmol/μg under non-diabetic conditions, $P = 0.015$; 1.90 ± 0.13 compared with 0.91 ± 0.07 nmol/μg under diabetic conditions, $P = 0.005$). However, diabetic A-FABP KO mice exhibited only a slightly higher NO production when compared with the respective WT mice (1.20 ± 0.08 compared with 0.78 ± 0.07 nmol/μg, $P = 0.05$) (Figure 5c). These data suggest that activation of the eNOS/NO pathway on MI/R or diabetes

induction was suppressed in the presence of A-FABP. To determine whether the beneficial effect of A-FABP deficiency on MI/R injury is attributable to the increased NO production, WT and A-FABP KO mice were pre-treated with either vehicle or the NOS inhibitor, L-NAME 1.5 mg/ml, followed by either diabetes induction or MI/R injury. The systolic arterial blood pressure of both WT and A-FABP KO mice was significantly increased to a similar extent after treatment with L-NAME, whereas diabetes induction with STZ did not affect arterial blood pressure in either type of mouse. Moreover, STZ did not further increase the systolic blood pressure of L-NAME-treated mice (see Supplementary Figure S5). Furthermore, the present data also show that treat-
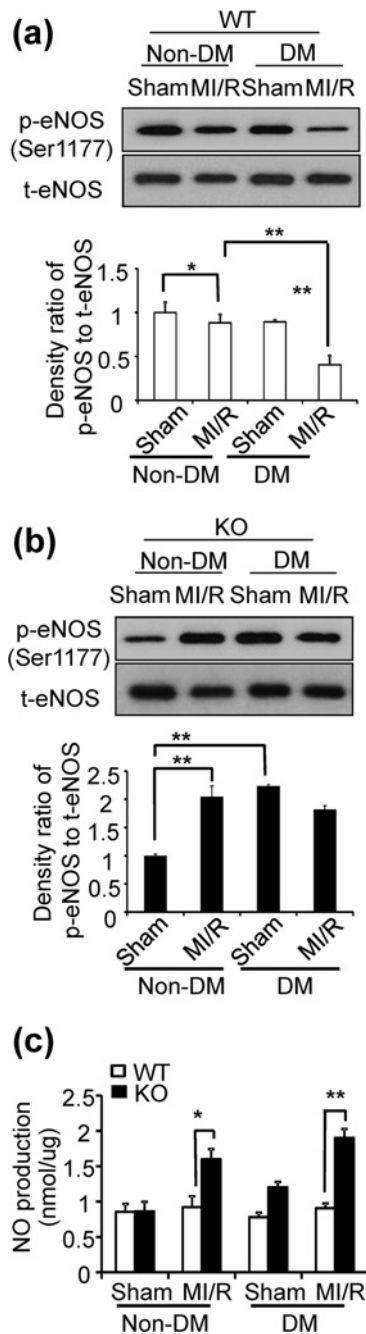
Figure 5 A-FABP deficiency protects against MI/R-induced cardiac injury through activation of the eNOS/NO pathway
Western blots measuring eNOS phosphorylation (Ser^{1177}) in heart tissues of (**a**) WT and (**b**) A-FABP KO mice. t-eNOS, total eNOS. (**c**) Cardiac NO production of A-FABP KO mice and WT mice. DM, diabetes mellitus. Values were expressed as means $\pm$ S.E.M.s. *$P < 0.05$, **$P < 0.01$; $n = 6$.

Figure 6 Treatment of NOS inhibitor abolishes the cardioprotective effects of A-FABP KO mice on MI/R injury
A-FABP KO mice and their WT littermates were treated with either vehicle (Veh) or L-NAME for 4 weeks, followed by MI/R injury or after diabetes induction. Effects of eNOS inhibition on MI/R-induced (**a**) myocardial infarction and (**b**) cardiac dysfunction. (**c**) Effect of eNOS inhibition on diabetes-induced cardiac dysfunction in A-FABP KO and WT mice. DM, diabetes mellitus. Values are expressed as means $\pm$ S.E.M. *$P < 0.05$, **$P < 0.01$; $n = 6$.

ment with L-NAME did not alter the MI/R- or diabetes-induced cardiac injury and function in WT mice (Figure 6). On the contrary, the beneficial effects of A-FABP deficiency on the alleviation of MI/R-induced myocardial infarction and deterioration of cardiac function were attenuated significantly when the A-FABP KO mice were treated with L-NAME (Figures 6a and 6b). How-
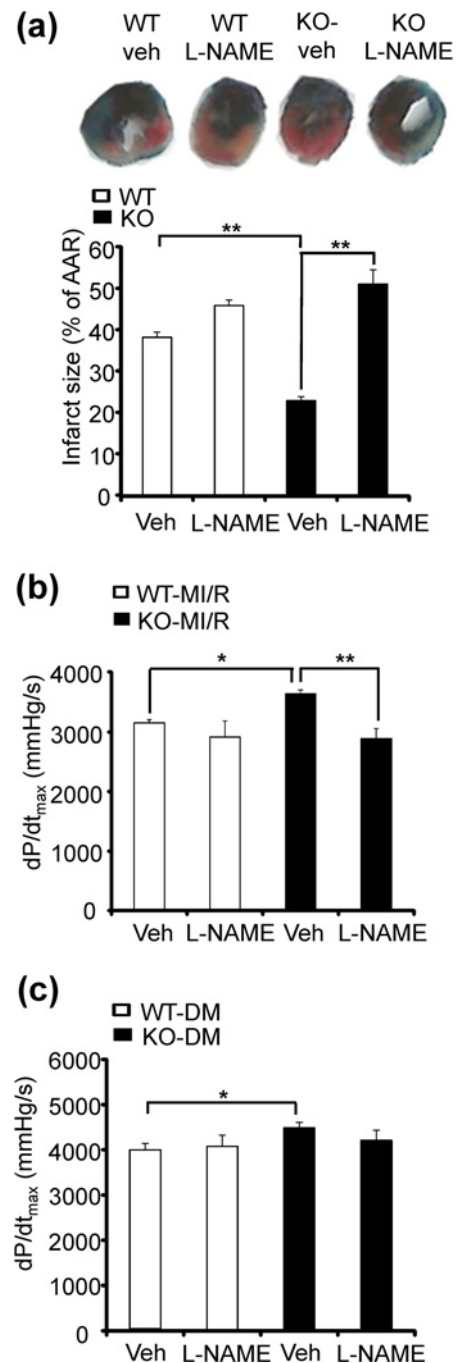
ever, NOS inhibition did not exaggerate diabetes-induced cardiac systolic dysfunction in A-FABP KO mice (Figure 6c). These data suggest that A-FABP deficiency protects against MI/R-induced

cardiac injury mainly because of increased NO production. However, increased NO production in the A-FABP-deficient heart did not contribute to the alleviation of diabetes-induced cardiac dysfunction.

To exclude other molecular sources that could be responsible for MI/R-induced increased NO production in A-FABP KO mice, the protein expression of iNOS was also determined. There was no significant change in iNOS expression after MI/R in either WT or A-FABP KO animals (see Supplementary Figure S6) which suggests that the elevated NO production in A-FABP KO mice mainly depends on eNOS activity.

DISCUSSION

A-FABP is recognized as a key mediator of various obesity-related cardiometabolic disorders [5]. Clinical and *in vitro* studies suggest that A-FABP is also implicated in cardiac dysfunction [12–15]. A-FABP-deficient mice are protected against diet-induced metabolic disorders such as insulin resistance, hyperlipidaemia and fatty liver despite their increased susceptibility to diet-induced obesity compared with WT mice [28]. Therefore, in the present study, a STZ-induced Type 1, rather than a diet-induced Type 2, diabetes model was established to investigate the role of A-FABP in MI/R-induced cardiac injury associated with the disease, and to minimize the metabolic discrepancy between WT and A-FABP KO mice on diabetes induction, which may affect MI/R injury.

The data in the present study show that endothelial cells were identified as the major cellular source of cardiac A-FABP, which is supported by our previous findings [19]. Both mRNA and protein expression of A-FABP were markedly increased in the cardiac tissues of STZ-exposed and/or MI/R-subjected mice, and the former exhibited a higher A-FABP expression than the latter. This induction of cardiac A-FABP was accompanied by an elevated circulating level of the adipokine. Under diabetic conditions, MI/R can only slightly but insignificantly enhance the expression of A-FABP in mice. This may be due to the severe induction of A-FABP expression by STZ-induced diabetes which masked the additive effect of MI/R.

A-FABP deficiency conferred cardioprotection with diminished infarct size and reduced cardiac apoptosis, and maintained better cardiac systolic and diastolic functions on MI/R-induced cardiac injury under both non-diabetic and diabetic conditions. The induction of NO production in A-FABP-deficient heart is specific for MI/R injury but not for diabetes induction. Moreover, treatment with the NOS inhibitor L-NAME attenuates the beneficial effect of A-FABP deficiency in alleviating MI/R-induced myocardial infarction and cardiac dysfunction, but not those induced by diabetes, although it exerts no effect on WT mice. These data suggest that the cardioprotective effect of A-FABP deficiency on MI/R injury is at least in part due to activation of the eNOS/NO pathway in endothelial cells, which subsequently alleviates cardiac oxidative stress and inflammation. Moreover, A-FABP deficiency protects against diabetes-induced cardiac dysfunction by attenuating superoxide anion production. Under

diabetic conditions, the presence of elevated superoxide anion further exaggerates MI/R-induced oxidative and nitrative stress and inflammation, leading to more severe cardiac damage and impairment of cardiac function. Thus, the findings of the present study provide *in vivo* evidence that A-FABP is involved in the development of MI/R- or diabetes-induced cardiac injury and dysfunction, as well as the exaggeration of MI/R-induced cardiac injury under diabetic condition. Consistent with previous findings [3,4], the data from the present study show that diabetes increases the susceptibility to MI/R-induced cardiac injury and that this can probably be attributed to the markedly enhanced expression of A-FABP.

Cardiomyocyte survival depends on capillary endothelial cells for a proper supply of oxygenated blood, and the expression and release of protective signals and a variety of autocrine and paracrine factors to maintain cardiac metabolism, growth and an appropriate coronary vascular diameter [17]. Endothelial dysfunction precedes most cardiovascular diseases and is implicated in cardiac dysfunction [18]. The bioavailability of NO synthesized from L-arginine by eNOS plays an obligatory role in the maintenance of proper endothelial function [29]. Patients with diabetes exhibit a reduced ability to generate NO from L-arginine [30] and are more susceptible to ischaemia/reperfusion injury compared with healthy controls [4]. Mice deficient in eNOS also show increased MI/R injury [31]. Conversely, genetic over-expression of eNOS or NO donors attenuate MI/R injury in mice [32,33]. The eNOS/NO pathway exerts various cardiovascular protective effects through the suppression of oxidative stress, inflammation and apoptosis [26]. Consistent with these findings, the present observation of elevated eNOS phosphorylation and increased NO production in the heart of A-FABP KO mice explains the protective effects of the deletion against MI/R injury.

Exogenous A-FABP and lipid-induced A-FABP expression decrease eNOS phosphorylation and NO production in cultured endothelial cells whereas pharmacological inhibition of A-FABP reverses the condition and improves endothelial function in ApoE KO mice [19,20] and prevents coronary endothelial dysfunction in the pig [21]. The findings of the present study demonstrate that A-FABP is expressed in cardiac endothelial cells but not in cardiomyocytes, and that this expression increases in response to acute MI/R injury and diabetes; this suggests that its adverse effect on endothelial cells contributes to cardiac dysfunction. Cardiac eNOS phosphorylation and NO production after MI/R were significantly reduced in WT mice, but both were augmented in A-FABP KO mice, an increase associated with reduced cardiac apoptosis and improved function. These data imply that a protective mechanism associated with the activation of eNOS in response to MI/R is suppressed in the presence of A-FABP, with a resultant decreased NO bioavailability, illustrating the development of endothelial dysfunction. This interpretation is helped by the observation that the beneficial effects of A-FABP deficiency were abolished by the administration of the eNOS inhibitor L-NAME.

Although eNOS can also be expressed in cardiomyocytes, the endothelium is the major contributor of eNOS-derived NO affecting myocardial contractility [34]. In the isolated rabbit heart, the

increase in myocardial NO production in response to mechanical stimulation is abrogated after removing cardiac endothelial and endocardial cells [35]. Furthermore, the inotropic response of cardiac ventricular myocytes to β-adrenergic stimulation necessitates the production of NO from the coronary microvascular endothelium [34,36]. These findings also support the interpretation that MI/R-induced cardiac dysfunction can be primarily attributed to the endothelial dysfunction caused by A-FABP-mediated alterations in the eNOS/NO pathway.

Endothelial dysfunction resulting from an impaired eNOS/NO pathway increases oxidative stress and inflammation, which further enhance the severity of the endothelial dysfunction. This vicious cycle and the additive effects eventually contribute to heart failure [29]. Elevated production of reactive oxygen species (ROS) on MI/R injury directly damages lipids, proteins and DNA, resulting in irreversible oxidative modifications [37] associated with increased apoptosis, cardiac hypertrophy and contractile dysfunction [38]. Elevated ROS also cause mitochondrial uncoupling, leading to cellular energy depletion in the diabetic heart [39]. ROS can interact with NO to generate nitrotyrosine, leading to severe nitrative stress and additional cardiac damage [40]. Superoxide anions scavenge NO and thus reduce NO bioavailability, contributing to endothelial dysfunction and apoptosis [41]. Hyperglycaemia-induced oxidative stress also enhances cardiac inflammation by activating the pro-inflammatory c-Jun N-terminal kinase (JNK) signalling pathway [42]. The results of the present study show that A-FABP KO mice exhibited an attenuated MI/R- and/or diabetes-induced cardiac ROS production. Reduced oxidative stress diminished nitrative stress in both the absence and the presence of diabetes, which may contribute to the subsequent alleviation of cardiac cell apoptosis and inflammation.

Pro-inflammatory cytokines also critically contribute to the pathogenesis of MI/R-induced injury. Elevated TNF-α and IL-6 promote cardiac hypertrophy, fibrosis and left ventricular dysfunction [43,44]. TNF-α and IL-1β increase epicardial thickness and induce cardiac contractile dysfunction [45]. A-FABP is a key mediator of inflammatory responses in macrophages [46,47] whereas both genetic disruption and pharmacological inhibition of A-FABP result in decreased production of pro-inflammatory cytokines [5]. However, in the present study, no macrophage infiltration was evidenced in the myocardium after acute MI/R injury and/or diabetes induction in either WT or A-FABP KO mice, and the cardiac expression of the macrophage marker F4/80 was also similar, suggesting that the attenuated cardiac inflammation in A-FABP KO mice after MI/R can be attributed mainly to the anti-inflammatory role of NO, the diminished ROS production in the myocardium on MI/R and diabetes induction, or the low systemic inflammatory state in A-FABP KO mice. The elevated expression of inflammatory cytokines in response to myocardial infarction may be contributed by cardiac fibroblasts and cardiomyocytes [48,49]. Exposure to cytokines is associated with induction of iNOS expression and activity mainly in infiltrated inflammatory cells [50]. However, there was no change in iNOS expression among groups in the present study, which may be due to a non-significant macrophage infiltration in the myocardium on short-term MI/R injury.

In conclusion, the present study provides the novel insight that A-FABP plays a critical role in the development of acute MI/R-induced cardiac dysfunction by inducing oxidative stress and inflammation primarily via the modulation of the eNOS/NO pathway in endothelial cells. Diabetes-induced elevation of A-FABP associated with raised superoxide anion production may account for its adverse effect on the exaggeration of MI/R-induced injury. These findings highlight the importance of A-FABP in the pathogenesis of cardiac disorders. In particular, they suggest that A-FABP may be a potential therapeutic target for the treatment of diabetes-associated cardiac complications.

CLINICAL PERSPECTIVES

- Circulating levels of A-FABP are elevated in patients with diabetes and closely associated with ischaemic heart disease, but the pathological link between diabetes and MI/R-induced cardiac injury remains unclear. The present study was designed to investigate the role of A-FABP in MI/R injury under non-diabetic and diabetic condition.

- Endothelial expression of A-FABP is increased on diabetes induction and acute MI/R. Elevated A-FABP expression plays a critical role in the development of acute MI/R injury by suppressing eNOS activation and NO production. Diabetes-induced elevation of A-FABP expression, associated with increased superoxide anion production, may contribute to the diabetes-induced cardiac dysfunction and the further exaggeration that it causes of MI/R-induced cardiac injury.

- A-FABP is a negative regulator of the eNOS/NO pathway causing endothelial dysfunction, which subsequently contributes to cardiac dysfunction by inducing oxidative stress and inflammation. A-FABP may be a potential therapeutic target for the treatment of diabetes-associated cardiac diseases.

REFERENCES

1 Go, A.S., Mozaffarian, D., Roger, V.L., Benjamin, E.J., Berry, J.D., Borden, W.B., Bravata, D.M., Dai, S., Ford, E.S., Fox, C.S. et al. (2013) Executive summary: heart disease and stroke statistics – 2013 update: a report from the American Heart Association. Circulation **127**, 143–152 CrossRef PubMed

2 Braunwald, E. and Kloner, R.A. (1985) Myocardial reperfusion: a double-edged sword? J. Clin. Invest. **76**, 1713–1719 CrossRef PubMed

3 Norhammar, A., Lindback, J., Ryden, L., Wallentin, L. and Stenestrand, U., Register of Information and Knowledge about Swedish Heart Intensive Care (2007) Improved but still high short- and long-term mortality rates after myocardial infarction in patients with diabetes mellitus: a time-trend report from the Swedish Register of Information and Knowledge about Swedish Heart Intensive Care Admission. Heart **93**, 1577–1583 CrossRef PubMed

4 Feuvray, D., Idell-Wenger, J.A. and Neely, J.R. (1979) Effects of ischemia on rat myocardial function and metabolism in diabetes. Circ. Res. **44**, 322–329 CrossRef PubMed

5 Furuhashi, M. and Hotamisligil, G.S. (2008) Fatty acid-binding proteins: role in metabolic diseases and potential as drug targets. Nat. Rev. Drug Discov. **7**, 489–503 CrossRef PubMed

6 Xu, A., Wang, Y., Xu, J.Y., Stejskal, D., Tam, S., Zhang, J., Wat, N.M., Wong, W.K. and Lam, K.S. (2006) Adipocyte fatty acid-binding protein is a plasma biomarker closely associated with obesity and metabolic syndrome. Clin. Chem. **52**, 405–413 CrossRef PubMed

7 Blaha, V., Musil, F., Smahelova, A., Ticha, A., Hyspler, R., Haluzik, M., Lesna, J. and Sobotka, L. (2012) Effects of body fat reduction on plasma adipocyte fatty acid-binding protein concentration in obese patients with type 1 diabetes mellitus. Neuro Endocrinol. Lett. **33** (Suppl. 2), 6–12 PubMed

8 Tso, A.W., Xu, A., Sham, P.C., Wat, N.M., Wang, Y., Fong, C.H., Cheung, B.M., Janus, E.D. and Lam, K.S. (2007) Serum adipocyte fatty acid binding protein as a new biomarker predicting the development of type 2 diabetes: a 10-year prospective study in a Chinese cohort. Diabetes Care **30**, 2667–2672 CrossRef PubMed

9 Veniant, M.M., Hale, C., Helmering, J., Chen, M.M., Stanislaus, S., Busby, J., Vonderfecht, S., Xu, J. and Lloyd, D.J. (2012) FGF21 promotes metabolic homeostasis via white adipose and leptin in mice. PLoS One **7**, e40164 CrossRef PubMed

10 Bao, Y., Lu, Z., Zhou, M., Li, H., Wang, Y., Gao, M., Wei, M. and Jia, W. (2011) Serum levels of adipocyte fatty acid-binding protein are associated with the severity of coronary artery disease in Chinese women. PLoS One **6**, e19115 CrossRef PubMed

11 von Eynatten, M., Breitling, L.P., Roos, M., Baumann, M., Rothenbacher, D. and Brenner, H. (2012) Circulating adipocyte fatty acid-binding protein levels and cardiovascular morbidity and mortality in patients with coronary heart disease: a 10-year prospective study. Arterioscler. Thromb. Vasc. Biol. **32**, 2327–2335 CrossRef PubMed

12 Baessler, A., Lamounier-Zepter, V., Fenk, S., Strack, C., Lahmann, C., Loew, T., Schmitz, G., Bluher, M., Bornstein, S.R. and Fischer, M. (2014) Adipocyte fatty acid-binding protein levels are associated with left ventricular diastolic dysfunction in morbidly obese subjects. Nutr. Diabetes **4**, e106 CrossRef PubMed

13 Lamounier-Zepter, V., Look, C., Alvarez, J., Christ, T., Ravens, U., Schunck, W.H., Ehrhart-Bornstein, M., Bornstein, S.R. and Morano, I. (2009) Adipocyte fatty acid-binding protein suppresses cardiomyocyte contraction: a new link between obesity and heart disease. Circ. Res. **105**, 326–334 CrossRef PubMed

14 Balci, M.M., Arslan, U., Firat, H., Kocaoglu, I., Vural, M.G., Balci, K.G., Maden, O., Gurbuz, O.A., Ardic, S. and Yeter, E. (2012) Serum levels of adipocyte fatty acid-binding protein are independently associated with left ventricular mass and myocardial performance index in obstructive sleep apnea syndrome. J. Investig. Med. **60**, 1020–1026 PubMed

15 Liu, M., Zhou, M., Bao, Y., Xu, Z., Li, H., Zhang, H., Zhu, W., Zhang, J., Xu, A., Wei, M. et al. (2013) Circulating adipocyte fatty acid-binding protein levels are independently associated with heart failure. Clin. Sci. (Lond.) **124**, 115–122 CrossRef PubMed

16 Djousse, L., Bartz, T.M., Ix, J.H., Kochar, J., Kizer, J.R., Gottdiener, J.S., Tracy, R.P., Mozaffarian, D., Siscovick, D.S., Mukamal, K.J. et al. (2013) Fatty acid-binding protein 4 and incident heart failure: the Cardiovascular Health Study. Eur. J. Heart Fail. **15**, 394–399 CrossRef PubMed

17 Brutsaert, D.L. (2003) Cardiac endothelial-myocardial signaling: its role in cardiac growth, contractile performance, and rhythmicity. Physiol. Rev. **83**, 59–115 CrossRef PubMed

18 Katz, S.D., Hryniewicz, K., Hriljac, I., Balidemaj, K., Dimayuga, C., Hudaihed, A. and Yasskiy, A. (2005) Vascular endothelial dysfunction and mortality risk in patients with chronic heart failure. Circulation **111**, 310–314 CrossRef PubMed

19 Lee, M.Y., Li, H., Xiao, Y., Zhou, Z., Xu, A. and Vanhoutte, P.M. (2011) Chronic administration of BMS309403 improves endothelial function in apolipoprotein E-deficient mice and in cultured human endothelial cells. Br. J. Pharmacol. **162**, 1564–1576 CrossRef PubMed

20 Aragones, G., Saavedra, P., Heras, M., Cabre, A., Girona, J. and Masana, L. (2012) Fatty acid-binding protein 4 impairs the insulin-dependent nitric oxide pathway in vascular endothelial cells. Cardiovasc. Diabetol. **11**, 72 CrossRef PubMed

21 Chan, C.K., Zhao, Y., Liao, S.Y., Zhang, Y.L., Lee, M.Y., Xu, A., Tse, H.F. and Vanhoutte, P.M. (2013) A-FABP and oxidative stress underlie the impairment of endothelium-dependent relaxations to serotonin and the intima-medial thickening in the porcine coronary artery with regenerated endothelium. ACS Chem. Neurosci. **4**, 122–129 CrossRef PubMed

22 Bae, S. and Zhang, L. (2005) Gender differences in cardioprotection against ischemia/reperfusion injury in adult rat hearts: focus on Akt and protein kinase C signaling. J. Pharmacol. Exp. Ther. **315**, 1125–1135 CrossRef PubMed

23 Tao, L., Gao, E., Jiao, X., Yuan, Y., Li, S., Christopher, T.A., Lopez, B.L., Koch, W., Chan, L., Goldstein, B.J. et al. (2007) Adiponectin cardioprotection after myocardial ischemia/reperfusion involves the reduction of oxidative/nitrative stress. Circulation **115**, 1408–1416 CrossRef PubMed

24 Hoo, R.L., Lee, I.P., Zhou, M., Wong, J.Y., Hui, X., Xu, A. and Lam, K.S. (2013) Pharmacological inhibition of adipocyte fatty acid binding protein alleviates both acute liver injury and non-alcoholic steatohepatitis in mice. J. Hepatol. **58**, 358–364 CrossRef PubMed

25 Lambert, J.M., Lopez, E.F. and Lindsey, M.L. (2008) Macrophage roles following myocardial infarction. Int. J. Cardiol. **130**, 147–158 CrossRef PubMed

26 Yu, Q., Gao, F. and Ma, X.L. (2011) Insulin says NO to cardiovascular disease. Cardiovasc. Res. **89**, 516–524 CrossRef PubMed

27 Reference deleted

28 Hotamisligil, G.S., Johnson, R.S., Distel, R.J., Ellis, R., Papaioannou, V.E. and Spiegelman, B.M. (1996) Uncoupling of obesity from insulin resistance through a targeted mutation in aP2, the adipocyte fatty acid binding protein. Science **274**, 1377–1379 CrossRef PubMed

29 Marti, C.N., Gheorghiade, M., Kalogeropoulos, A.P., Georgiopoulou, V.V., Quyyumi, A.A. and Butler, J. (2012) Endothelial dysfunction, arterial stiffness, and heart failure. J. Am. Coll. Cardiol. **60**, 1455–1469 CrossRef PubMed

30   Pieper, G.M. (1998) Review of alterations in endothelial nitric oxide production in diabetes: protective role of arginine on endothelial dysfunction. Hypertension **31**, 1047–1060 CrossRef PubMed

31   Scherrer-Crosbie, M., Ullrich, R., Bloch, K.D., Nakajima, H., Nasseri, B., Aretz, H.T., Lindsey, M.L., Vancon, A.C., Huang, P.L., Lee, R.T. et al. (2001) Endothelial nitric oxide synthase limits left ventricular remodeling after myocardial infarction in mice. Circulation **104**, 1286–1291 CrossRef PubMed

32   Brunner, F., Maier, R., Andrew, P., Wolkart, G., Zechner, R. and Mayer, B. (2003) Attenuation of myocardial ischemia/reperfusion injury in mice with myocyte-specific overexpression of endothelial nitric oxide synthase. Cardiovasc. Res. **57**, 55–62 CrossRef PubMed

33   Lefer, A.M. and Lefer, D.J. (1996) The role of nitric oxide and cell adhesion molecules on the microcirculation in ischaemia-reperfusion. Cardiovasc. Res. **32**, 743–751 CrossRef PubMed

34   Seddon, M., Shah, A.M. and Casadei, B. (2007) Cardiomyocytes as effectors of nitric oxide signalling. Cardiovasc. Res. **75**, 315–326 CrossRef PubMed

35   Pinsky, D.J., Patton, S., Mesaros, S., Brovkovych, V., Kubaszewski, E., Grunfeld, S. and Malinski, T. (1997) Mechanical transduction of nitric oxide synthesis in the beating heart. Circ. Res. **81**, 372–379 CrossRef PubMed

36   Godecke, A., Heinicke, T., Kamkin, A., Kiseleva, I., Strasser, R.H., Decking, U.K., Stumpe, T., Isenberg, G. and Schrader, J. (2001) Inotropic response to beta-adrenergic receptor stimulation and anti-adrenergic effect of ACh in endothelial NO synthase-deficient mouse hearts. J. Physiol. **532**, 195–204 CrossRef PubMed

37   Finkel, T. (2003) Oxidant signals and oxidative stress. Curr. Opin. Cell Biol. **15**, 247–254 CrossRef PubMed

38   Grieve, D.J. and Shah, A.M. (2003) Oxidative stress in heart failure. More than just damage. Eur. Heart J. **24**, 2161–2163 CrossRef PubMed

39   Boudina, S., Sena, S., O'Neill, B.T., Tathireddy, P., Young, M.E. and Abel, E.D. (2005) Reduced mitochondrial oxidative capacity and increased mitochondrial uncoupling impair myocardial energetics in obesity. Circulation **112**, 2686–2695 CrossRef PubMed

40   Beckman, J.S. and Koppenol, W.H. (1996) Nitric oxide, superoxide, and peroxynitrite: the good, the bad, and ugly. Am. J. Physiol. **271**, C1424–C1437 PubMed

41   Cai, H. and Harrison, D.G. (2000) Endothelial dysfunction in cardiovascular diseases: the role of oxidant stress. Circ. Res. **87**, 840–844 CrossRef PubMed

42   Tibbles, L.A. and Woodgett, J.R. (1999) The stress-activated protein kinase pathways. Cell. Mol. Life Sci. **55**, 1230–1254 CrossRef PubMed

43   Sun, M., Dawood, F., Wen, W.H., Chen, M., Dixon, I., Kirshenbaum, L.A. and Liu, P.P. (2004) Excessive tumor necrosis factor activation after infarction contributes to susceptibility of myocardial rupture and left ventricular dysfunction. Circulation **110**, 3221–3228 CrossRef PubMed

44   Kaneko, K., Kanda, T., Yokoyama, T., Nakazato, Y., Iwasaki, T., Kobayashi, I. and Nagai, R. (1997) Expression of interleukin-6 in the ventricles and coronary arteries of patients with myocardial infarction. Res. Commun. Mol. Pathol. Pharmacol. **97**, 3–12 PubMed

45   Lorenzo, O., Picatoste, B., Ares-Carrasco, S., Ramirez, E., Egido, J. and Tunon, J. (2011) Potential role of nuclear factor kappaB in diabetic cardiomyopathy. Mediators Inflamm. **2011**, 652097 CrossRef PubMed

46   Makowski, L., Boord, J.B., Maeda, K., Babaev, V.R., Uysal, K.T., Morgan, M.A., Parker, R.A., Suttles, J., Fazio, S., Hotamisligil, G.S. et al. (2001) Lack of macrophage fatty-acid-binding protein aP2 protects mice deficient in apolipoprotein E against atherosclerosis. Nat. Med. **7**, 699–705 CrossRef PubMed

47   Hui, X., Li, H., Zhou, Z., Lam, K.S., Xiao, Y., Wu, D., Ding, K., Wang, Y., Vanhoutte, P.M. and Xu, A. (2010) Adipocyte fatty acid-binding protein modulates inflammatory responses in macrophages through a positive feedback loop involving c-Jun NH2-terminal kinases and activator protein-1. J. Biol. Chem. **285**, 10273–10280 CrossRef PubMed

48   Porter, K.E. and Turner, N.A. (2009) Cardiac fibroblasts: at the heart of myocardial remodeling. Pharmacol. Ther. **123**, 255–278 CrossRef PubMed

49   Aoyagi, T. and Matsui, T. (2011) The cardiomyocyte as a source of cytokines in cardiac injury. J. Cell Sci. Ther. **2012**, 003 PubMed

50   Fukuchi, M., Hussain, S.N. and Giaid, A. (1998) Heterogeneous expression and activity of endothelial and inducible nitric oxide synthases in end-stage human heart failure: their relation to lesion site and beta-adrenergic receptor therapy. Circulation **98**, 132–139 CrossRef PubMed